anomolous dispersion for all non-hydrogen atoms were included in $F$ by using the values of Cromer and Ibers[26] for $\Delta f'$ and $\Delta f''$.

The positions of the iron atoms were established from a three-dimensional Patterson function calculated from all the intensity data, and the remaining non-hydrogen atoms were located from successive Fourier difference maps. The positions of several hydrogen atoms were calculated; these values were included in the refinement for a few cycles and thereafter held fixed. Anisotropic thermal parameters were introduced for the two iron atoms, but the remaining atoms were refined isotropically. The error in an observation of unit weight was 2.71, and the largest parameter shift in the final cycle of refinement was 0.08 times the estimated standard deviation.

The model converged with $R = 0.112$ and $R_w = 0.112$, where $R = \sum ||F_o| - |F_c||/\sum |F_o|$ and $R_w = (\sum w(|F_o| - |F_c|)^2/\sum w|F_o|^2)^{1/2}$. Tables of observed and calculated structure factors, positional and thermal parameters, and mean planes are available (see supplementary material paragraph). The computer system and programs are described elsewhere.[27]

**Supplementary Material Available:** Tables of calculated and observed structure factors, positional and thermal parameters, and calculated least-squares planes (9 pages). Ordering information is given on any current masthead page.

(26) Cromer, D. T.; Ibers, J. A., in ref 24.

(27) Freyberg, D. P.; Mockler, G. M.; Sinn, E. *J. Chem. Soc., Dalton Trans.* **1976**, 447.

# Oxygenation Patterns for Substituted *meso*-Tetraphenylporphyrin Complexes of Iron(II). Spectroscopic Detection of Dioxygen Complexes in the Absence of Amines

**Lechoslaw Latos-Grazynski, Ru-Jen Cheng, Gerd N. La Mar, and Alan L. Balch***

*Contribution from the Department of Chemistry, University of California, Davis, California 95616. Received January 22, 1982*

**Abstract:** The reaction of dioxygen with iron(II) porphyrins in inert solvents has been studied by $^1$H NMR spectroscopy in order to detect the presence of reactive intermediates. Sterically hindered porphyrins have been examined in which the formation of peroxo- and oxo-bridged dimeric structure is limited. The iron(II) porphyrins studied have $^1$H NMR spectra characteristic of intermediate-spin ($S = 1$), four-coordinate species. Reduction of [*meso*-tetrakis(2,4,6-trimethoxyphenyl)porphyrin]iron(III) chloride ([T(2,4,6-MeO)$_3$PP]Fe$^{III}$Cl) or [*meso*-tetrakis(2,4,6-triethoxyphenyl)porphyrin]iron(III) chloride ([T(2,4,6-EtO)$_3$PP]Fe$^{III}$Cl) with either aqueous sodium dithionite or zinc amalgam in dichloromethane solution produces [T(2,4,6-MeO)$_3$PP]Fe$^{II}$ or [T(2,4,6-EtO)$_3$PP]Fe$^{II}$. The previously reported reduction of these two porphyrins with piperidine has been reexamined and shown to form the bis(piperidine) adducts of the iron(II) porphyrins. Addition of dioxygen to paramagnetic [*meso*-tetrakis($\alpha,\alpha,\alpha,\alpha$-*o*-pivalamidophenyl)porphyrin]iron(II) ([TpivPP]Fe$^{II}$) in toluene solution below $-70$ °C produces a new diamagnetic complex that is formulated as [TpivPP]FeO$_2$. $^1$H NMR spectroscopic observations indicated that, on warming, this species is successively converted to [TpivPP]Fe$^{III}$O$_2$Fe$^{III}$[TpivPP] and to [TpivPP]Fe$^{III}$OFe$^{III}$[TpivPP]. The latter has been previously isolated. Reaction of [TpivPP]FeO$_2$ with *N*-methylimidazole (*N*-MeIm) at $-70$ °C results in the formation of (*N*-MeIm)[TpivPF]FeO$_2$. Addition of dioxygen to [T(3,4,5-MeO)$_3$PP]Fe$^{II}$ at $-70$ °C in toluene solution results in the formation of diamagnetic [T(3,4,5-MeO)$_3$PP]FeO$_2$. This, on warming, is converted to [T(3,4,5-MeO)$_3$PP]FeO$_2$Fe[T(3,4,5-MeO)$_3$PP] and then to [T(3,4,5-MeO)$_3$PP]FeOH and [T(3,4,5-MeO)$_3$PP]FeOFe[T(3,4,5-MeO)$_3$PP] as the final stable products. Addition of dioxygen to [T(2,4,6-MeO)$_3$PP]Fe$^{II}$ and [T(2,4,6-EtO)$_3$PP]Fe$^{II}$ in dichloromethane solution at $-70$ °C produces diamagnetic dioxygen adducts. On warming, these undergo dissociation to form the parent iron(II) complex and irreversible oxidation to form iron(III) porphyrin hydroxide and chloride.

The reactions of dioxygen with iron(II) porphyrins have been intensively studied.[1-5] The conditions necessary to obtain reversible coordination of dioxygen, rather than irreversible oxidation to produce iron(III) porphyrins, have received particular attention. The extraordinary attention given to reversible coordination arises because reversible binding is required for the operation of the dioxygen transport and storage proteins, hemoglobin and myoglobin.[6] In synthetic systems, reversible dioxygen binding involves a ligand exchange reaction (eq 1) in which dioxygen replaces another axial ligand. Usually the axial ligand is a heterocyclic



$$\text{(1)}$$
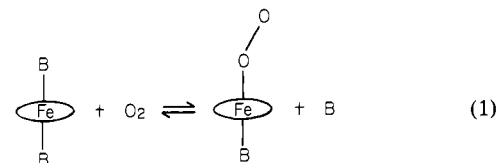
amine, pyridine, or *N*-methylimidazole.

In the absence of an axial base, PFe$^{II}$[7] reacts with dioxygen to produce the antiferromagnetic $\mu$-oxo dimer PFeOFeP as the ultimate product. The probable pathway leading to this product is shown in eq 2. We have undertaken examination of this process utilizing high-field $^1$H NMR spectroscopy to detect the iron

(1) James, B. R. "The Porphyrins"; Dolphin, D., Ed.; Academic Press: New York, 1978; Vol. 5, pp 205–302.

(2) Jones, P. D.; Summerville, D. A.; Basolo, F. *Chem. Rev.* **1979**, *79*, 139–178.

(3) Collman, J. P. *Acc. Chem. Res.* **1977**, *10*, 265–272.

(4) Collman, J. P.; Halpert, T. R.; Suslick, K. S. In "Metal Ion Activation of Dioxygen"; Spiro, T. G., Ed.; Wiley: New York, 1980; pp 1–72.

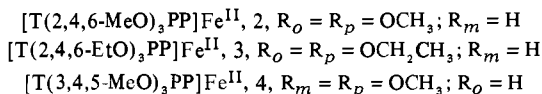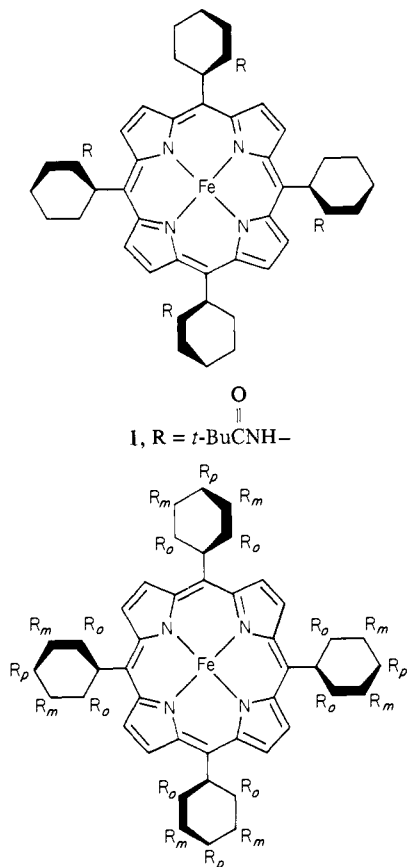(5) Traylor, T. G. *Acc. Chem. Res.* **1981**, *14*, 102–109.

(6) Perutz, M. F. *Annu. Rev. Biochem.* **1979**, *48*, 327–386.

(7) Abbreviations used are: P, porphyrin dianions; H$_2$[TpivPP], *meso*-tetrakis($\alpha,\alpha,\alpha,\alpha$-*o*-pivalamidophenyl)porphyrin; H$_2$[T(2,4,6-MeO)$_3$PP], *meso*-tetrakis(2,4,6-trimethoxyphenyl)porphyrin; H$_2$[T(2,4,6-Et)$_3$PP], *meso*-tetrakis(2,4,6-triethoxyphenyl)porphyrin; B, amine base; *N*-MeIm, *N*-methylimidazole; pip, piperidine.

$$2 \quad \overset{O}{\underset{}{\overset{\|}{O}}} \diagdown Fe \qquad (2)$$
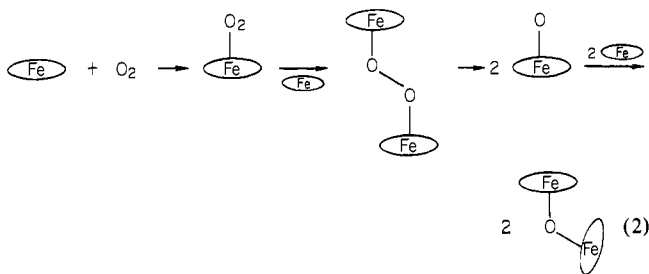
porphyrin species present and low temperature to control the rate of reaction. These conditions have allowed us to directly observe previously undetected reaction intermediates. The peroxo-bridged intermediate (PFeOOFeP) has been characterized by recording both its $^1$H NMR and electronic spectra in the temperature range $-80$ to $-20$ °C.[8,9] The mechanism of conversion of this anti-ferromagnetically coupled dimer to PFeOFeP has been examined.[9] Reaction of PFeOOFeP with amines (B) has been shown to produce BPFeO, which may also be directly detected in the temperature range $-80$ to $20$ °C.[10] BPFeO, which contains the ferryl unit $(FeO)^{2+}$, has been shown to be capable of oxygen atom transfer to substrates such as triphenylphosphine.[11]

Here we present results on the oxygenation of solutions of a number of phenyl-substituted derivatives of [TPP]Fe$^{II}$ at low temperatures. The porphyrin complexes involved are 1-4. These



O
‖
**1,** R = *t*-BuCNH−



[T(2,4,6-MeO)$_3$PP]Fe$^{II}$, **2**, R$_o$ = R$_p$ = OCH$_3$; R$_m$ = H

[T(2,4,6-EtO)$_3$PP]Fe$^{II}$, **3**, R$_o$ = R$_p$ = OCH$_2$CH$_3$; R$_m$ = H

[T(3,4,5-MeO)$_3$PP]Fe$^{II}$, **4**, R$_m$ = R$_p$ = OCH$_3$; R$_o$ = H

porphyrins possess varying degrees of steric protection that limit the formation of dimeric structures to some extent. Complex **1**, of course, is hindered on one side only, while the other porphyrins are hindered on both sides of the porphyrin plane. These steric constraints limit the formation of oxo- and peroxo-bridged complexes. While [TpivPP]Fe has been converted to [TpivPP]-Fe$^{III}$OFe$^{III}$[TpivPP],[12] it has been reported that **2** and **3** cannot form $\mu$-oxo dimers.[13-15] We have shown that iron(III) hydroxy complexes can be prepared by treating [T(2,4,6-MeO)$_3$PP]Fe$^{III}$Cl and [T(2,4,6-EtO)$_3$PP]Fe$^{III}$Cl with sodium hydroxide, while similar treatment of [T(3,4,5-MeO)$_3$PP]Fe$^{III}$Cl produces a mixture of PFe$^{III}$OH and PFe$^{III}$OFe$^{III}$P.[16]

By carrying out the oxygenation of the iron(II) complexes **1-4** at low temperatures in inert solvents (toluene or dichloromethane), it is possible to detect various intermediates during the oxygenation reaction. In particular, we show that the complexes **1-4** all form diamagnetic dioxygen complexes at ca. $-70$ °C in the absence of the heterocyclic amine that usually occupies the coordination site trans to the dioxygen ligand.

## Results

**Characterization of Unligated PFe$^{II}$.** The PFe$^{II}$ species utilized in this study have been prepared by in situ reduction of the PFe$^{III}$Cl species. Two reducing agents, aqueous sodium dithionite[17,18] and zinc amalgam, have been used. Each produces the same PFe$^{II}$ species. The reductions have been followed by both electronic and $^1$H NMR spectroscopy. Identical spectral changes are seen with either reduction technique. $^1$H NMR parameters for the iron(II) complexes are contained in Table I. The patterns of resonances found are consistent, in all cases, with the presence of planar, four-coordinate iron(II) ($S = 1$) in all of these porphyrins. The assignment of resonances follows directly from the assignments previously made on simpler porphrins.[18]

As an example we consider the spectral properties of [T-(2,4,6-MeO)$_3$PP]Fe$^{II}$ and [T(2,4,6-EtO)$_3$PP]Fe$^{II}$. These deserve particular attention because it has been previously claimed that reduction of [T(2,4,6-MeO)$_3$PP]FeCl and [T(2,4,6-EtO)$_3$PP]FeCl by piperidine produces diamagnetic, four-coordinate iron(II) complexes.[13-15] Because of presumed steric inhibition, piperidine was not believed capable of axial coordination to the iron in these protected porphyrins.

The electronic spectral changes that accompany the reduction of [T(2,4,6-EtO)$_3$PP]Fe$^{III}$Cl to [T(2,4,6-EtO)$_3$PP]Fe$^{II}$ by dithionite are shown in traces A and B of Figure 1. The spectrum shown in trace B is typical of that of a four-coordinate iron(II) porphyrin. Similar spectral changes are seen for the reduction of [T(2,4,6-MeO)$_3$PP]Fe$^{III}$Cl.

The $^1$H NMR spectra of [T(2,4,6-MeO)$_3$PP]Fe$^{II}$ and [T-(2,4,6-EtO)$_3$PP]Fe$^{II}$ in dichloromethane-$d_2$ solutions are shown in Figure 2. These spectra are similar to those of [TPP]Fe$^{II}$ and other unligated PFe$^{II}$ species that have been examined previously.[18] Assignments of resonances in this figure have been made by comparison with the spectra of other iron(II) porphyrins, by consideration of the spin–spin splitting observed, and by consideration of the relative intensities of the resonances. A Curie plot for [T(2,4,6-MeO)$_3$PP]Fe$^{II}$ in dichloromethane solution is shown in Figure 3. The pattern of resonances and their temperature-dependent behavior, particularly the non-zero intercept of the pyrrole proton, are characteristic of four-coordinate $S = 1$ iron(II) porphyrin complexes.

(8) Chin, D.-H.; Del Gaudio, J.; La Mar, G. N.; Balch, A. L. *J. Am. Chem. Soc.* **1977**, *99*, 5486–5488.

(9) Chin, D.-H.; La Mar, G. N.; Balch, A. L. *J. Am. Chem. Soc.* **1980**, *102*, 4344–4350.

(10) Chin, D.-H.; Balch, A. L.; La Mar, G. N. *J. Am. Chem. Soc.* **1980**, *102*, 1446–1448.

(11) Chin, D.-H.; La Mar, G. N.; Balch, A. L. *J. Am. Chem. Soc.* **1980**, *102*, 5946–5947.

(12) Collman, J. P.; Gagne, R. R.; Reed, C. A.; Halbert, T. R.; Lang, G.; Robinson, W. T. *J. Am. Chem. Soc.* **1975**, *97*, 1427–1439.

(13) Vaska, L.; Amundsen, A. R.; Brady, R.; Flynn, B. R.; Nakni, H. *Finn. Chem. Lett.* **1974**, 66–67.

(14) Amundsen, A. R.; Vaska, L. *Inorg. Chim. Acta* **1975**, *14*, 49–51.

(15) Amundsen, A. R. Ph.D. Thesis, Clarkson College of Technology, 1976.

(16) Cheng, R.-J.; Latos-Grazynski, L.; Balch, A. L. *Inorg. Chem.* **1982**, *21*, 2412–2418.

(17) Brault, D., Rougee, M. *Biochemistry* **1974**, *13*, 4598.

(18) Goff, H.; La Mar, G. N.; Reed, C. A. *J. Am. Chem. Soc.* **1977**, *99*, 3641–3646.

Table I.   $^1$H NMR Chemical Shifts for Iron Porphyrins

| compound[a] | temp, °C | chemical shifts, ppm | | | |
|---|---|---|---|---|---|
| | | pyrrole | ortho | meta | para |
| [TpivPP]Fe$^{II}$ | 25 | 3.2 | 0.0$^c$ | 14.3, 12.0 | 12.9 |
| [T(2,4,6-MeO)$_3$PP]Fe$^{II}$ $^b$ | 25 | 2.2 | 3.5 | 11.1 | 7.1 |
| [T(2,4,6-EtO)$_3$PP]Fe$^{II}$ $^b$ | 25 | 1.6 | 5.0$^e$, −3.9$^d$ | 10.5 | 7.2$^e$, 3.5$^d$ |
| [T(3,4,5-MeO)$_3$PP]Fe$^{II}$ | 25 | 4.0 | 21.7 | 6.3 | 7.8 |
| [TpivPP]FeO$_2$ | −76 | 8.2 | 0.44$^c$ | 9.69 | |
| [T(2,4,6-MeO)$_3$PP]FeO$_2$ $^b$ | −75 | 9.0 | 3.6 | 6.6 | 4.1 |
| [T(2,4,6-EtO)$_3$PP]FeO$_2$ $^b$ | −75 | 9.1 | 3.9$^e$, 0.7$^d$ | 6.5 | 4.2$^e$, 1.5$^d$ |
| [T(3,4,5-MeO)$_3$PP]FeO$_2$ | −75 | 9.8 | 7.4 | 3.3 | 4.2 |
| ([TpivPP]Fe)$_2$O$_2$ | −25 | 16.6 | −0.1$^c$ | 9.7 | |
| ([T(3,4,5-MeO)$_3$PP]Fe)$_2$O$_2$ | −30 | 16.8 | | 3.2, 4.1 | 4.2 |
| ([TpivPP]Fe)$_2$O | 25 | 13.7 | | 3.2, 4.2 | 4.2 |
| ([T(3,4,5-MeO)$_3$PP]Fe)$_2$O | 25 | 13.6 | −0.3$^c$ | 9.21 | |
| [T(2,4,6-EtO)$_3$PP]Fe(CO)$_2$ | 25 | 8.77 | 3.88$^e$, 0.55$^d$ | 6.55 | 4.29$^e$, 1.58$^d$ |
| [T(2,4,6-EtO)$_3$PP]Fe(CO) | 25 | 8.61 | 3.87$^e$, 0.56$^d$ | 6.53, 6.54 | 4.28$^e$, 1.58$^d$ |
| [T(3,4,5-MeO)$_3$PP]Fe(CO)$_2$ | 25 | 9.21 | 7.53 | 3.50 | 4.17 |

$^a$ Solvent is toluene-$d_8$ unless noted.   $^b$ Solvent is dichloromethane-$d_2$.   $^c$ *tert*-Butyl resonance only is given.   $^d$ Methyl groups.   $^e$ Methylene group.





**Figure 2.** $^1$H NMR spectra of CD$_2$Cl$_2$ solution of (A) [T(2,4,6-MeO)$_3$PP]Fe$^{II}$ and (B) [T(2,4,6-EtO)$_3$PP]Fe$^{II}$ at 25 °C and 200 MHz. The resonance assignments are shown: (q) 1:4:4:1 quartet; (t) 1:3:1 triplet; (*) solvent resonances.
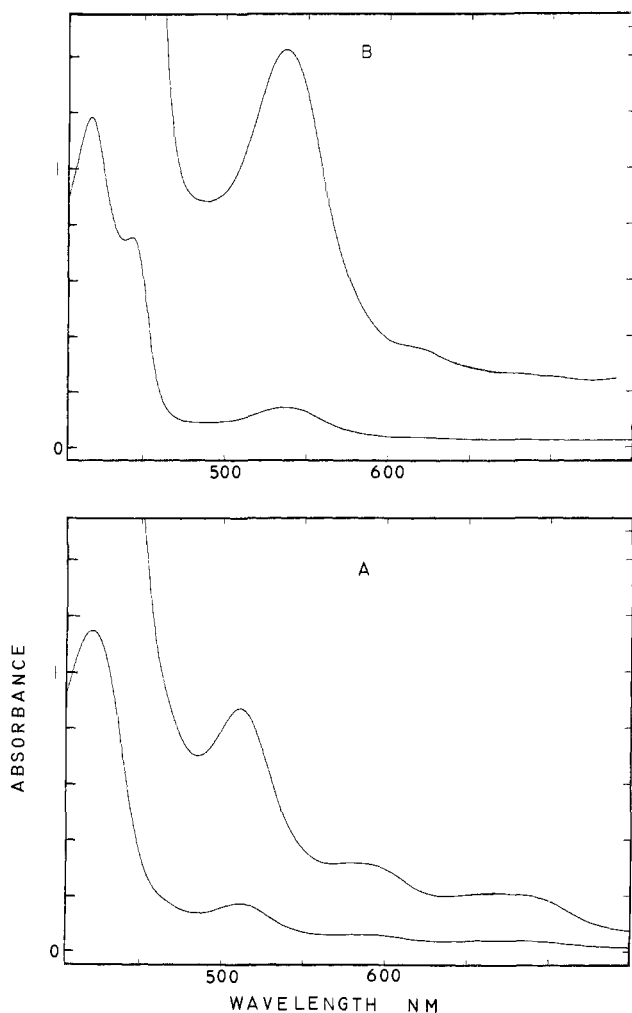


**Figure 1.** Electronic spectra of dichloromethane solutions of (A) [T-(2,4,6-EtO)PP]Fe$^{III}$Cl and (B) [T(2,4,6-EtO)$_3$PP]Fe$^{II}$ prepared by dithionite reduction of [T(2,4,6-EtO)$_3$PP]Fe$^{II}$. The concentration of iron was 1.0 × 10$^{-4}$ M, and the cell path length was 1.0 mm. The absorbance scale is expanded 5× in A and 10× in B for the portion of the spectrum shown on the right.

The orientation of the ortho phenyl substituents with respect to the iron can be estimated from the $^1$H NMR spectra. The location of these groups is important because it has been claimed that they severely inhibit not only dimerization through bridging ligands but also access of other ligands to the iron atom. Previous analysis of the $^1$H NMR spectra of [TPP]Fe$^{II}$ and its para-sub-
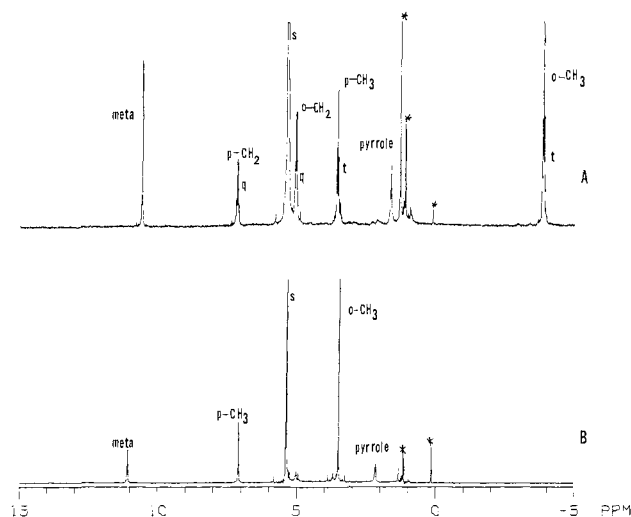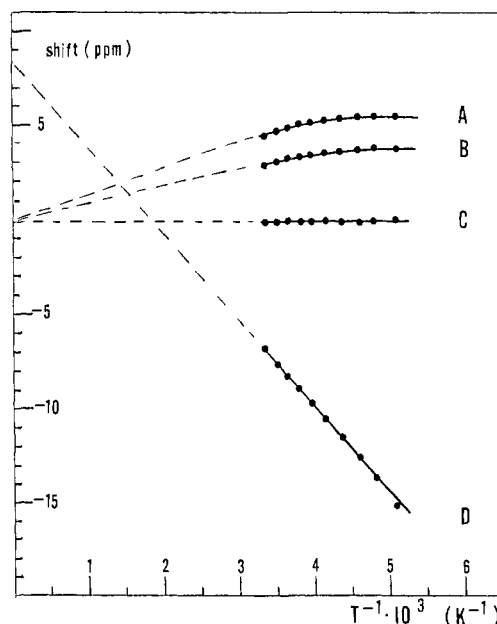
**Figure 3.** Curie plot for [T(2,4,6-MeO)$_3$PP]Fe$^{II}$ in dichloromethane solution: (A) meta phenyl protons; (B) para methoxy protons; (C) ortho methoxy protons; (D) pyrrole protons.
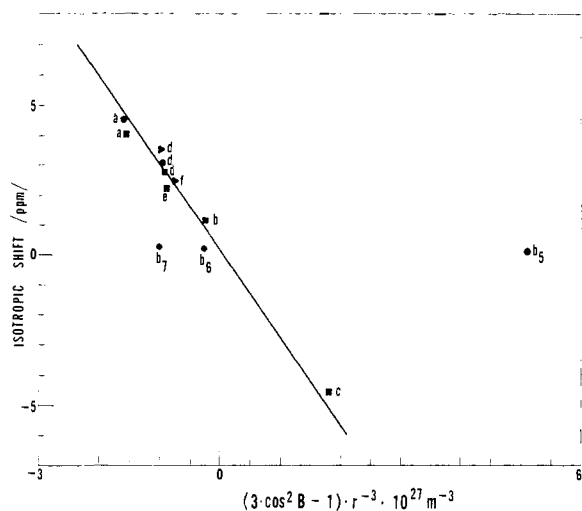
**Figure 4.** Plot of isotropic shifts for meso phenyl substituents vs. the calculated geometric factors $(3 \cos^2 \theta - 1)r^{-3}$. The straignt line is plotted directly from Figure 4 of ref 18. Circles, $[T(2,4,6\text{-MeO})_3PP]Fe^{II}$; squares, $[T(2,4,6\text{-EtO})_3PP]Fe^{II}$; triangles, $[T(3,4,5\text{-MeO})_3PP]Fe^{II}$. Proton labels are (a) meta protons, (b) ortho $OCH_2$ or $OCH_3$, (c) ortho $OCH_2CH_3$, (d) para $OCH_2$ or $OCH_3$, (e) para $OCH_2CH_3$, (f) meta $OCH_3$.

stituted derivatives has indicated that the phenyl protons' shifts originate in an essentially wholly dipolar interaction.[18] This has been quantitatively confirmed by single-crystal magnetic susceptibility measurements.[19] The dipolar shift for axial symmetry is given[20] by

$$\left(\frac{\Delta H}{H}\right)_{\text{dip}} = -\frac{1}{3N}(X_{\|} - X_{\perp})\frac{3 \cos^2\theta - 1}{r^3}$$

A plot of isotopic shifts for phenyl substituents as a function of calculated geometric factors $(3 \cos^2 \theta - 1)r^{-3}$ for $[TPP]Fe^{II}$ and para-substituted derivatives shows good linear correlation.[18] Relevant data for complexes **2**, **3**, and **4** are plotted in Figure 4. The solid line in the figure is taken directly from ref 16, and the new data points are shown individually. The geometric factors have been computed in standard fashion assuming that the phenyl groups are perpendicular to the porphyrin plane. Particular attention was given to the orientation of the *o*-methyl groups in $[T(2,4,6\text{-MeO})_3PP]Fe^{II}$. Geometric factors have been computed for a freely rotating methyl group in each of the three locations specified in **5–7**. (In both **5** and **6** the methyl carbon lies in the
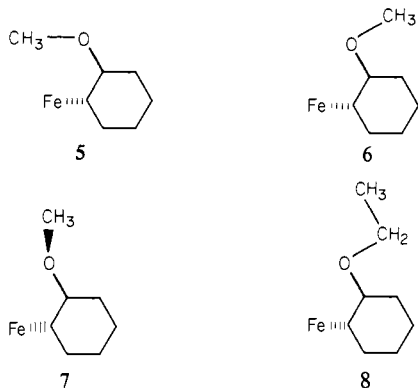


phenyl plane, while in **7**, the $C_{Me}$–O–$C_{Ph}$ plane is perpendicular to the phenyl plane.) The points corresponding to orientations **5**, **6**, and **7** are labeled $b_5$, $b_6$, and $b_7$ in Figure 4. From the
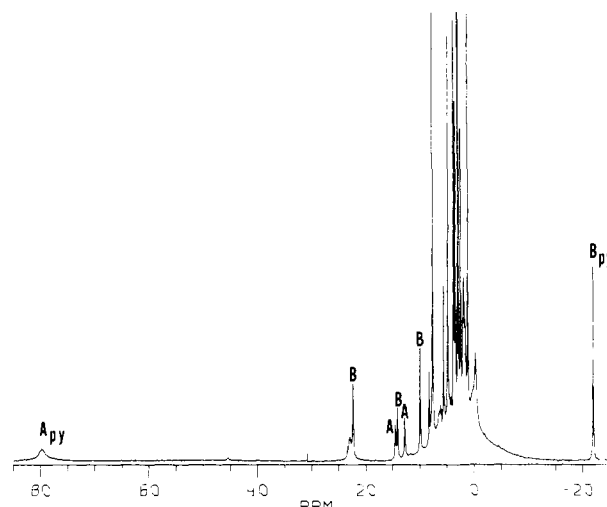
**Figure 5.** $^1H$ NMR spectrum at 360 MHz of a solution of $[T(2,4,6\text{-}EtO)_3PP]Fe^{III}Cl$ in the presence of a large excess of pyridine. Peaks labeled A are due to $[T(2,4,6\text{-EtO})_3PP]Fe^{III}Cl$; those labeled B are due to $[[T(2,4,6\text{-EtO})_3PP]Fe^{III}(pip)_2]Cl$. Subscript py denotes the characteristic pyrrole protons.



**Figure 5.** $^1H$ NMR spectrum at 360 MHz of a solution of $[T(2,4,6\text{-}EtO)_3PP]Fe^{III}Cl$ in the presence of a large excess of pyridine. Peaks labeled A are due to $[T(2,4,6\text{-EtO})_3PP]Fe^{III}Cl$; those labeled B are due to $[[T(2,4,6\text{-EtO})_3PP]Fe^{III}(pip)_2]Cl$. Subscript py denotes the characteristic pyrrole protons.
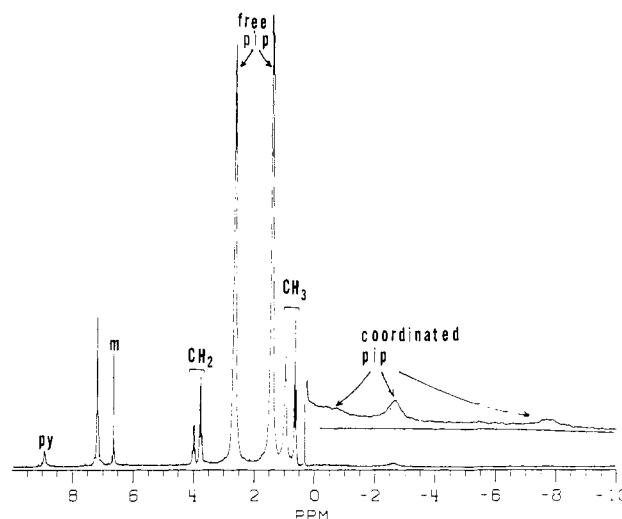


**Figure 6.** 360-MHz $^1H$ NMR spectrum of a solution of $[T(2,4,6\text{-}EtO)_3PP]Fe^{II}(pip)_2$ in benzene-$d_6$ obtained by allowing $[T(2,4,6\text{-}EtO)_3PP]Fe^{III}Cl$ to react with excess piperidine under anaerobic conditions.

proximity of these points to the line, we conclude that, on average, the methoxy group is bent away from the iron and it spends relatively little time in orientation **5** where it would most effectively block the axial ligation of the iron atom. For $[T(2,4,6\text{-}EtO)_3PP]Fe^{II}$, the computed geometric factors used in Figure 4 refer to a single orientation (**8**).

In order to evaluate the earlier claim of the formation of diamagnetic, four-coordinate $[T(2,4,6\text{-MeO})_3PP]Fe^{II}$ and $[T(2,4,6\text{-EtO})_3PP]Fe^{II}$ by piperidine reduction,[13–15] we reexamined the reaction of piperidine with these iron porphyrins by $^1H$ NMR spectroscopy.[21,22] Addition of excess piperidine to $[T(2,4,6\text{-}EtO)_3PP]Fe^{III}Cl$ produces the spectrum shown in Figure 5. Two species are detected. The unreacted $[T(2,4,6\text{-EtO})_3PP]Fe^{III}Cl$ is readily identified. The other new resonances are consistent with the spectrum expected for low-spin six-coordinate iron(III) complex $[[T(2,4,6\text{-EtO})_3PP]Fe(pip)_2]Cl$. The upfield pyrrole resonance and resonances in the region 10–25 ppm, due to the axial

(19) Boyd, P. D. W.; Buckingham, D. A.; McMeeking, R. F.; Mitra, S. *Inorg. Chem.* **1979**, *18*, 3585–3591.

(20) Jesson, J. P. In "NMR of Paramagnetic Molecules"; La Mar, G. N.; Horrocks, W. D., Jr.; Holm, R. H., Eds.; Academic Press: New York, 1973; Chapter 1.

(21) Piperdine reduction of $PFe^{III}Cl$ has frequently been used to form $PFe^{II}(pip)_2$. Epstein, L. M.; Straub, D. K., Maricondi, C. *Inorg. Chem.* **1967**, *6*, 1720.

(22) Del Gaudio, J.; La Mar, G. N. *J. Am. Chem. Soc.* **1978**, *100*, 1112–1119.
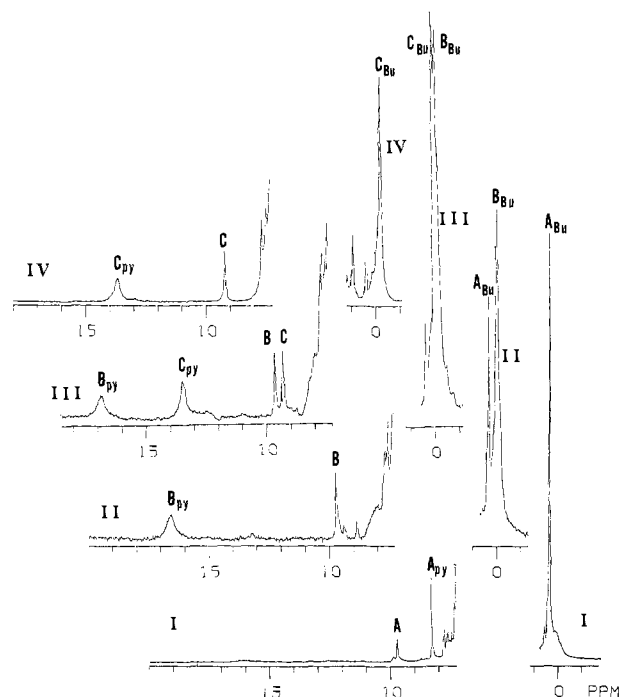
**Figure 7.** 360-MHz $^1$H NMR spectra of a toluene-$d_6$ solution of [TpivPP]Fe$^{II}$ that has been exposed to excess dioxygen at -75 °C: (Trace I) sample at -75 °C, (II) sample at -25 °C, (III) sample at -12 °C, (IV) sample at 25 °C. Resonance due to individual species are denoted by capital letters as follows: (A) [TpivPP]FeO$_2$, (B) [TpivPP]FeO$_2$Fe-[TpivPF], (C) [TpivPP]FeOFe[TpivPP]. Subscripts refer to resonances assignements as follows: (py) pyrrole protons, (Bu) *tert*-butyl protons, (Ph) phenyl protons.

piperidine ligands, are characteristic of such species.[23] The relative amounts of [T(2,4,6-EtO)$_3$PP]Fe$^{III}$Cl and [[T(2,4,6-EtO)$_3$PP]-Fe$^{III}$(pip)$_2$]Cl depend on the concentration of piperidine, and with a large enough excess of piperidine present, it is possible to form [[T(2,4,6-EtO)$_3$PP]Fe$^{III}$(pip)$_2$]Cl exclusively. On standing under anaerobic conditions, [[T(2,4,6-EtO)$_3$PP]Fe$^{III}$(pip)$_2$]Cl, in the presence of excess piperidine, undergoes reduction to form diamagnetic [T(2,4,6-EtO)$_3$PP]Fe$^{II}$(pip)$_2$. The $^1$H NMR spectrum of this diamagnetic complex is shown in Figure 6. The upfield resonances between 0 and -10 ppm are due to coordinated piperidine shifted by ring-current effects. The spectrum may be compared to that of [TPP]Fe$^{II}$(pip)$_2$ shown in Figure 2 of ref 22. An identical spectrum with that of Figure 5 can be obtained by adding piperidine to preformed [T(2,4,6-EtO)$_3$PP]Fe$^{II}$. Similar observations have been made with T(2,4,6-MeO)$_3$PPFe$^{III}$Cl. Consequently, it is clear that piperidine does reduce these iron(II) porphyrins as expected, but contrary to previous expectations, piperidine is capable of coordination to both the iron(III) and iron(II) complexes. Previous claims[13-15] of having isolated diamagnetic, four-coordinate iron porphyrins are in error; the species isolated were PFe$^{II}$(pip)$_2$.

The possibility of coordination of the ether oxygens to the iron in the PFe$^{II}$ species **2**, **3**, and **4** has been considered. Structural constraints require that if ether oxygen coordination were to occur, it would be intermolecular in nature. Five-coordinate iron(II) porphyrins exhibit pyrrole resonances in the range -50 to -52 ppm,[24,25] while six-coordinate iron(II) porphyrins are generally diamagnetic. Thus ether coordination should manifest itself in significant shifts in the position of the pyrrole resonances. However, the locations of the pyrrole resonances in [T(2,4,6-MeO)$_3$PP]Fe$^{II}$ and [T(2,4,6-EtO)$_3$PP]Fe$^{II}$, as well as their tem-

perature dependences, are inconsistent with any significant amount of ether oxygen coordination to iron.

**Oxygenation of [TpivPP]Fe$^{II}$.  1.** Addition of dioxygen to a toluene solution of [TpivPP]Fe$^{II}$ at -76 °C produces a new, diamagnetic iron porphyrin, TpivPPFeO$_2$. The formation of this species is readily detected by the changes observed in the $^1$H NMR spectra shown in Figure 7. Trace I shows the spectrum after the addition of excess dioxygen. No [TpivPP]Fe$^{II}$ remains at this point, but a new species (A) is present. The presence of A is verified by the presence of a sharp peak at 0.3 ppm, which is assigned to the *tert*-butyl protons. Additional resonances due to the adduct are also observable in the region 9-10 ppm. The formation of the dioxygen adduct A at -80 °C appears to be irreversible. The adduct A is stable toward repeated freeze-pump-thaw cycles and to flushing with nitrogen gas as long as the sample is maintained at -80 °C or lower temperatures.

Gradual warming of the sample of A produces an interesting series of spectral changes. A spectrum recorded at -25 °C is shown in trace II of Figure 7. Some of the initial adduct A is still present because the *tert*-butyl resonances at 0.3 ppm remains. However, additional resonances appear at 0, 9.8, and 16.5 ppm. The simultaneous growth and decay of these three resonances indicate that they are caused by a single new species (B). Further warming to 12 °C produces additional changes, which are shown in trace III of Figure 7. At this point three species, A, B, and C, are present. The new species (C) is characterized by a broad resonance at 13.3 ppm and narrow resonances at 9.2 and -0.3 ppm. C is identified as [TpivPP]FeOFe[TpivPP] by comparison with the $^1$H NMR spectra of other oxo-bridged porphyrin dimers[26] and an authentic sample.[12] Inspection of these spectra allows the resonance at 13 ppm to be assigned to the pyrrole protons, the resonance at 9.2 ppm to be assigned to the phenyl protons, and the resonance at -0.3 ppm to be assigned to the *tert*-butyl protons. Further warming of the sample results in the loss in intensity of both the intermediate species A and B so that eventually only [TpivPP]FeOF[TpivPP] remains, as shown in trace IV of Figure 7.[26]

The intermediate B may be confidently identified as the peroxy-bridged complex [TpivPP]FeOOFe[TpivPP]. The broad resonance at ~16 ppm in the spectrum of B appears in the same region as the pyrrole resonance of [TPP]FeOOFe[TPP].[8,10] Moreover, the temperature-dependent behavior of this resonance, which shifts from ~16 ppm at -75 °C to ~17 ppm at -12 °C, is a clear indication of antiferromagnetic behavior, a characteristic of oxo- and peroxo-bridged iron(III) porphyrins. The larger anisotropic shift for the pyrrole resonance for B relative to [TpivPP]FeOFe[TpivPP] is also a characteristic that is shared by other related pairs of peroxo-bridged dimers and oxo-bridged dimers. Additionally, the line widths of all resonances assigned to the peroxo-bridged dimer are larger than the corresponding line widths of the oxo-bridged dimer. This is a consequence of the smaller antiferromagnetic coupling present in the peroxo-bridged dimer.[9] Finally, the conversion of PFeOOFeP into PFeOFeP has been demonstrated for other (*meso*-tetraphenyl-porphyrin)iron complexes.[10]

The formation of intermediate A has been independently confirmed by measurements of the optical spectra of these porphyrins. At -70 °C in dioxygen-free toluene solution, [TpivPP]Fe$^{II}$ displays an absorption band at 536 nm with a shoulder at 560 nm. Addition of dioxygen causes this band to shift so that the maximum now appears at 545 nm. Warming the solution results in further changes, so that at 25 °C the spectrum of [TpivPP]-FeOFe[TpivPP] (575 nm) is obtained.

As expected for a diamagnetic species, there is no ESR spectrum associated with the formation of A.

The intermediate A has been converted into (*N*-MeIm)-[TpivPP]FeO$_2$, the extensively characterized dioxygen adduct, which is stable at room temperature.[12,27] Relevant $^1$H NMR spectral data are shown in Figure 8. Trace I shows the downfield

(23) Satterlee, J. D.; La Mar, G. N.; Frye, J. S. *J. Am. Chem. Soc.* **1976**, *98*, 7275-7282.

(24) Goff, H.; La Mar, G. N. *J. Am. Chem. Soc.* **1977**, *99*, 6599-6606.

(25) In addition to PFe$^{II}$L species where L is an amine,[21] complexes where L contains an oxygen donor, i.e., triphenylphosphine oxide, also show the same pattern of shifts with pyrrole resonances in the range -50 to -52 ppm. Latos-Grazynski, L.; La Mar, G. N.; Balch, A. L., unpublished observations.

(26) La Mar, G. N.; Eaton, G. R.; Holm, R. H.; Walker, F. A. *J. Am. Chem. Soc.* **1973**, *95*, 63-75.

(27) Jameson, G. B.; Rodley, G. A.; Robinson, W. T.; Gagne, R. R.; Reed, C. A.; Collman, J. P. *Inorg. Chem.* **1978**, *17*, 850-857.
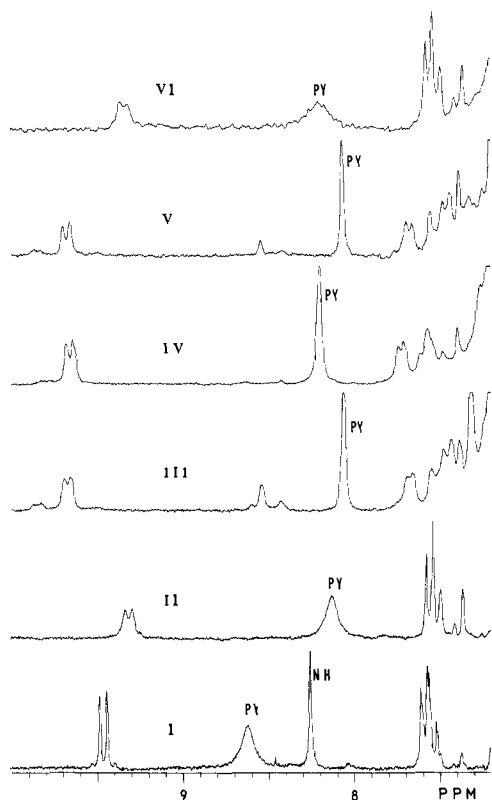
**Figure 8.** $^1$H NMR spectra at 360 MHz of: (I) [TpivPP]Fe$^{II}$(N-MeIm)$_2$ and excess N-MeIm at 25 °C; (II) the same solution as in I with 1 atm of dioxygen present at 25 °C, (N-MeIm)[TpivPP]FeO$_2$ is present; (III) the same solution as II but cooled to –75 °C, (N-MeIm)[TpivPP]FeO$_2$ is the principal species present; (IV) a solution of [TpivPP]Fe$^{II}$ at –75 °C to which excess dioxygen has been added, [TpivPP]FeO$_2$ is present; (V) the same solution shown in IV after the addition of N-MeIm at –75 °C; (VI) the same solution shown in V after warming to 25 °C. Position of the single resonance seen for the *tert*-butyl groups under these conditions: (I) 1.07 ppm, (II) 0.97 ppm, (III) 1.0 ppm, (IV) 0.44 ppm, (V) 1.0 ppm, (VI) 0.97 ppm.

portion of the spectrum of [TpivPP]Fe$^{II}$ in the presence of N-methylimidazole at 25 °C in toluene-$d_8$ solution. The porphyrin complex present is [TpivP]Fe$^{II}$(N-MeIm)$_2$. Trace II shows the spectrum of the same sample after dioxygen has been added. The new spectral features are ascribed to the formation of (N-MeIm)[TpivPP]FeO$_2$. Trace III shows the spectrum of this solution after it has been cooled to –70 °C. In traces IV–VI, the order of these operations is reversed. In trace IV the spectrum of intermediate A formed by adding excess dioxygen to [TpivPP]Fe$^{II}$ at –70 °C is shown. After addition of N-methylimidazole to this solution, the spectrum shown in trace V is produced. Warming this solution to 25 °C results in the spectral changes that are shown in trace VI. The similarities of the spectra in traces II and IV and in traces III and V are particularly significant. They demonstrate that a common product is formed regardless of the order of addition of N-methylimidazole and dioxygen to [TpivPP]Fe$^{II}$, so long as the addition of dioxygen is made at –70 °C and the solution is kept at that temperature until the heterocyclic amine is added. The difference between traces IV and V demonstrates the addition of N-methylimidazole to [TpivPF]FeO$_2$. The spectral changes shown in Figure 8 are accompanied by other changes in the remaining portion of the $^1$H NMR spectra. In particular, the *tert*-butyl resonances also show changes that serve to characterize the set of transformations described above. The position of the *tert*-butyl resonance is also indicated in the figure caption of Figure 8. The difference in thermal stability of (N-MeIm)[TpivPP]FeO$_2$ and [TpivPP]FeO$_2$ clearly demonstrates the role of the axial ligand in stabilizing the dioxygen adduct and preventing irreversible oxidation to form iron(III). Chart I summarizes the chemical transformations of [TpivPP]Fe$^{II}$.
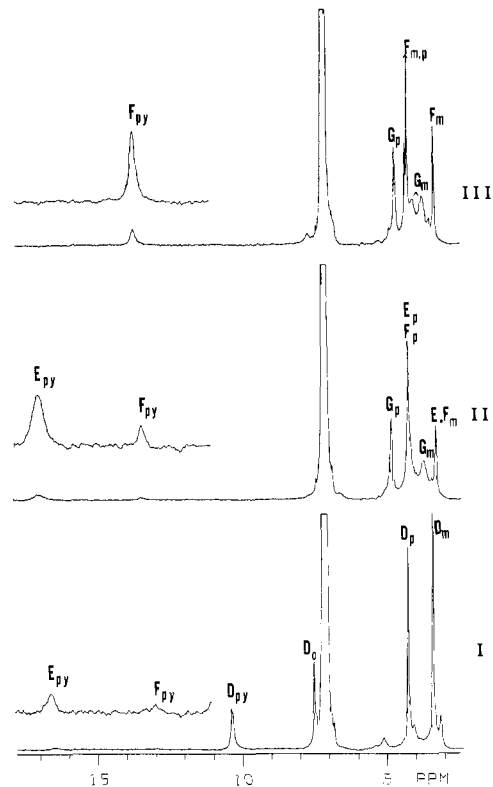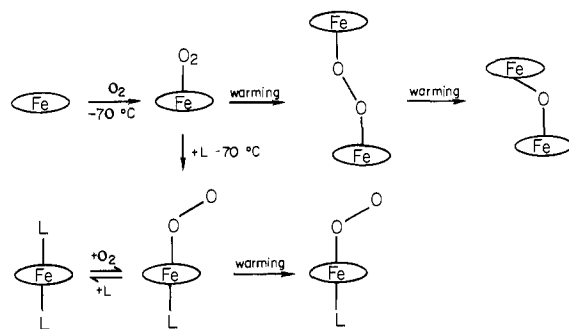


**Figure 9.** $^1$H NMR spectra of [T(3,4,5-MeO)$_3$PP]Fe$^{II}$ in the presence of excess dioxygen in toluene-$d_8$ solution: (I) after addition of dioxygen at –75 °C and warming to –60 °C, (II) after warming to 10 °C, (III) after warming to 25 °C.

**Chart I**



**Oxygenation of [T(3,4,5-MeO)$_3$PP]Fe$^{II}$.** Addition of dioxygen to a solution of [T(3,4,5-MeO)$_3$PP]Fe$^{II}$ in toluene-$d_8$ at or below –70 °C produces a series of $^1$H NMR spectral changes that parallel those found for [TpivPP]Fe$^{II}$. At the lowest temperatures, a diamagnetic species (D) is formed. The $^1$H NMR spectrum of D is shown in trace I of Figure 9. This spectrum is temperature dependent, as shown in Figure 10. At –90 °C three methoxy resonances are observed. On warming to –60 °C, two of the methoxy resonances broaden and then coalesce into a single resonance. Meanwhile, the other methoxy resonance remains unaltered in chemical shift and line width. These changes are reversed upon cooling back to –90 °C. The splitting of the meta methoxy resonances at low temperature is indicative of unsymmetrical coordination about the porphyrin plane, and the reversible temperature changes in the NMR spectrum are ascribed to the transfer of a dioxygen ligand from one side of the porphyrin plane to the other (eq 3). This could occur by either an associative
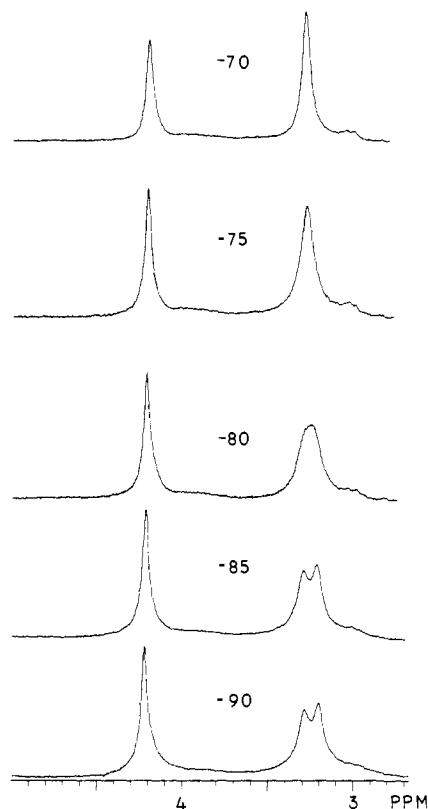


(3)
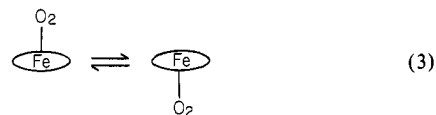
**Figure 10.** Methyl region of the 360-MHz spectrum of [T(3,4,5-MeO)$_3$PP]FeO$_2$ (intermediate D) in toluene-$d_8$ solution as a function of temperature. The changes are reversible.

or a dissociative process, and examples of both mechanisms have been discovered for five-coordinate iron porphyrin complexes.[28] At present, the available data do not establish the mechanism for the process shown in eq 3. This process is also observed with [T(2,4,6-MeO)$_3$PP]FeO$_2$, as described in the next section.

Further warming of this species irreversibly converts D into a second unstable intermediate (E), which is readily observed in trace II of Figure 9. E is identified as the peroxo-bridged complex [T(3,4,5-MeO)$_3$PP]FeO$_2$Fe[T(3,4,5-MeO)$_3$PP]. It has a pyrrole resonance that shifts from 16.4 ppm at −75 °C to 17.1 ppm at 10 °C. The chemical shift of this resonance and its temperature dependence, which is characteristic of an antiferromagnetically coupled species, are consistent with analogous properties of other peroxo-bridged iron porphyrin dimers.[10] Warming the oxygenated sample of [T(3,4,5-MeO)$_3$PP]Fe$^{II}$ to room temperature causes E to decay and two species, F([T(3,4,5-MeO)$_3$PP]FeOH) and G([T(3,4,5-MeO)$_3$PP]FeOFe[T(3,4,5-MeO)$_3$PP], to form. These two iron(III) complexes have been independently prepared by treating [T(3,4,5-MeO)$_3$PP]FeCl with aqueous sodium hydroxide. Generally this treatment results in the formation of PFeOFeP.[29] However, in the present case, a high-spin iron(III) species, the hydroxy complex is formed as well as the μ-oxo dimer. Further characterization of the hydroxy complex is presented elsewhere.[16]

**Oxygenation of [T(2,4,6-EtO)$_3$PP]Fe$^{II}$ and [T(2,4,6-MeO)$_3$PP]Fe$^{II}$.** The oxygenation of [T(2,4,6-MeO)$_3$PP]Fe$^{II}$ and [T(2,4,6-EtO)$_3$PP]Fe$^{II}$ had to be carried out in dichloromethane solution because these two complexes lack sufficient solubility in toluene solution.[30] Both complexes behaved similarly, but the
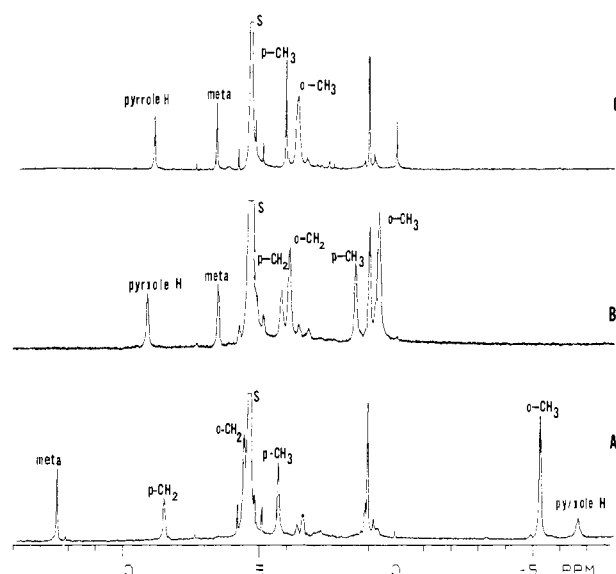
(28) Snyder, R. V.; La Mar, G. N. *J. Am. Chem. Soc.* **1976**, *98*, 4419–4424.

(29) Fleischer, E. B.; Srivastava, T. S. *J. Am. Chem. Soc.* **1969**, *91*, 2403–2405.

(30) The differences in oxygenation behavior of these two iron(II) porphyrins from other iron(II) porphyrins cannot be ascribed to solvent effects. TPPFeO$_2$FeTPP can be prepared in dichloromethane as well as in toluene so long as the dichloromethane is free of acidic impurities. Likewise, the formation of [TpivPP]FeO$_2$ and its conversion into [TpivPP]FeOFe[TpivPP] have also been observed in dichloromethane solution.

**Figure 11.** 200-MHz $^1$H NMR spectra of dichloromethane-$d_2$ solutions of: (A) [T(2,4,6-EtO)$_3$PP]Fe$^{II}$ at −75 °C, (B) [T(2,4,6-EtO)$_3$PP]Fe$^{II}$ and excess dioxygen at −75 °C, (C) [T(2,4,6-MeO)$_3$PP]Fe$^{II}$ and excess dioxygen at −75 °C.

ethoxy derivative has higher solubility.

Addition of dioxygen to either iron(II) complex at −80 °C results in the disappearance of the spectrum of the original iron(II) porphyrin and the formation of a new diamagnetic species H. The 200-MHz $^1$H NMR spectrum of the dioxygen adducts H of both [T(2,4,6-MeO)$_3$PP]Fe$^{II}$ and [T(2,4,6-EtO)$_3$PP]Fe$^{II}$ are shown in Figure 11 along with the assignments, which are based on comparison with other diamagnetic metalloporphyrins. The temperature-dependent $^1$H NMR spectra in the region of the meta phenyl and methoxy protons at 360 MHz are shown in Figure 12. Of particular significance are the observations of two resonances for the meta phenyl protons and three resonances for methoxy protons. This pattern of resonances is indicative of the presence of an unsymmetrical coordination about the porphyrin plane. In particular, this pattern is consistent with the formation of an adduct with one dioxygen ligand, [T(2,4,6-MeO)$_3$PP]FeO$_2$, and inconsistent with the formation of an adduct involving two equivalent dioxygen ligands, [T(2,4,6-MeO)$_3$PP]Fe(O$_2$)$_2$. Results on carbon monoxide complexes (vida infra) show that diamagnetic adducts of the types PFeL and PFeL$_2$ are distinguishable on the basis of their $^1$H NMR spectra.

As the solution is warmed, the spectrum of H undergoes a series of changes that do not correspond to the changes observed when [TpivPP]FeO$_2$ or [T(3,4,5-MeO)$_3$PP]FeO$_2$ are warmed. With [T(2,4,6-MeO)$_3$PP]FeO$_2$ and [T(2,4,6-EtO)$_3$PP]FeO$_2$ there is no evidence for the conversion into either a peroxo- or an oxo-bridged species. The ortho substituents effectively block the requisite close approach of the porphyrins.

The initial change upon warming a sample of [T(2,4,6-MeO)$_3$PP]FeO$_2$ is shown in Figure 12. The two meta phenyl proton resonances broaden and coalesce to give a single resonance. Similarly, two of the three methoxy proton resonances broaden and then coalesce. Further warming produces striking shifts in some of the resonance positions, but all resonances remain distinct. The temperature dependence of the proton resonances observed when a sample of [T(2,4,6-EtO)$_3$PP]FeO$_2$ is warmed in the presence of excess dioxygen is shown in Figure 13. The pattern of shifts observed for [T(2,4,6-MeO)$_3$PP]FeO$_2$ is similar. In the high-temperature limit, the spectrum approaches that of [T-(2,4,6-EtO)$_3$PP]Fe$^{II}$. Along with these changes, however, we also observe the slow formation of high-spin iron(III) porphyrins. These are detected by the growth of resonances in the region −120 to −80 ppm, which is characteristic of the pyrrole protons of PFe$^{III}$X.
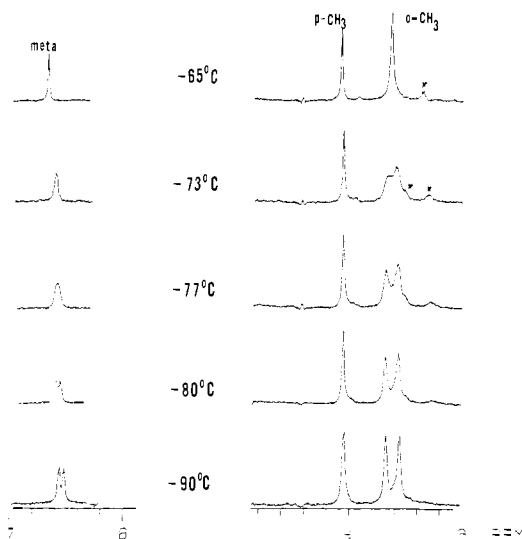
The temperature-dependent changes observed in the $^1$H NMR

**Figure 12.** Temperature dependence of the 360-MHz $^1H$ NMR spectrum of the meta protons and the methoxy protons of [T(2,4,6-MeO)$_3$PP]FeO$_2$.



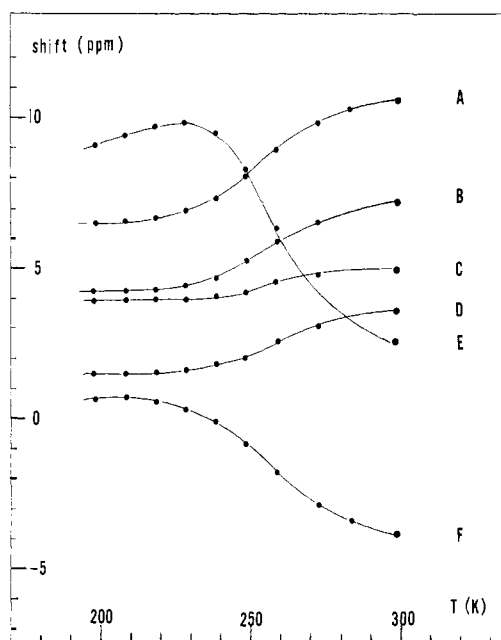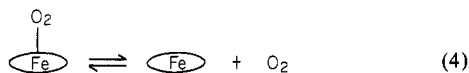**Figure 13.** Temperature dependence of the chemical shifts of [T(2,4,6-EtO)$_3$PP]Fe$^{II}$ in dichloromethane-$d_2$ solution under 1 atm of dioxygen. The individual proton resonances are identified as follows: (A) meta phenyl, (B) para methylene, (C) ortho methylene, (D) para methyl, (E) pyrrole, (F) ortho methyl.

spectra in Figure 13 are attributed to the reversible dissociation of dioxygen shown in eq 4.[31,32] At room temperature the spectrum

$$\underset{Fe}{\overset{O_2}{\diamond}} \rightleftharpoons \underset{Fe}{\diamond} + O_2 \qquad (4)$$

of [T(2,4,6-EtO)$_3$PP]Fe$^{II}$ or [T(2,4,6-MeO)$_3$PP]Fe$^{II}$ should be

unaffected by the addition of dioxygen. In fact the $^1H$ NMR spectra of both of these iron(II) complexes are observed unchanged when dioxygen is added. However, there is a slow disappearance of the spectrum of PFe$^{II}$ and an accompanying growth of resonances due to two high-spin iron complexes, PFeCl and PFeOH. Similarly, as the dioxygen adducts are warmed, in addition to the alteration in chemical shifts in Figure 13, a gradual loss in intensity of that part of the spectrum occurs. Simultaneously, there is the growth of resonances due to high-spin iron complexes.

**Addition of Carbon Monoxide.** Carbon monoxide adds readily to [T(2,4,6-EtO)$_3$PP]Fe$^{II}$ and [T(2,4,6-MeO)$_3$PP]Fe$^{II}$ at 25 °C to produce diamagnetic species. With [T(2,4,6-EtO)$_3$PP]Fe$^{II}$, both [T(2,4,6-EtO)$_3$PP]Fe(CO) and [T(2,4,6-EtO)$_3$PP]Fe(CO)$_2$ form. $^1H$ NMR spectral parameters are shown in Table I. The two adducts are easily distinguishable. [T(2,4,6-EtO)$_3$PP]Fe(CO) displays two equally intense meta phenyl proton resonances and three equally intense methyl and methylene resonances, while [T(2,4,6-EtO)$_3$PP]Fe(CO)$_2$ shows only one meta phenyl proton resonance and two methyl and methylene resonances in an intensity ratio of 2:1. At 25 °C the resolution of the two separate sets of resonances indicates that the two adducts are in slow exchange. The relative intensities of the resonances of the two species indicate that the two species are present in about equal proportions under 1 atm of carbon monoxide. Under similar conditions, the formation of [TPP]Fe(CO) and [TPP]Fe(CO)$_2$ in about equal proportions has been reported.[33]

Addition of carbon monoxide to [T(3,4,5-MeO)$_3$PP]Fe$^{II}$ proceeds to give only [T(3,4,5-MeO)$_3$PP]Fe(CO)$_2$. The $^1H$ NMR parameters are given in Table I. No evidence for the formation of [T(3,4,5-MeO)$_3$PP]Fe(CO) has been found. It has been reported that some ortho-substituted tetraphenylporphrin complexes of iron(II) also only produce six-coordinate carbon monoxide adducts.[34] The factors responsible for this behavior remain to be explored.

**Conclusions**

The observations recorded here indicate a consistent pattern of behavior of the iron(II) complexes 1–4 upon oxygenation. The initial formation of a diamagnetic dioxygen adduct is found for each of these porphyrins. The observations of inequivalent meta methoxy resonances in [T(3,4,5-MeO)$_3$PP]FeO$_2$ and inequivalent meta phenyl proton and ortho methoxy resonances in [T(2,4,6-MeO)$_3$PP]FeO$_2$ are consistent with the presence of a single dioxygen ligand in these species. For intermediate A, formed from [TpivPP]Fe$^{II}$ and dioxygen, we presume that only a single dioxygen ligand is present by analogy with other systems. The side of the porphyrin plane on which the dioxygen ligand resides in A has not been determined. A can be transformed into (N-MeIm)-[TpivPP]FeO$_2$ in which the oxygen lies on the side surrounded by the pickets while the imidazole ligand coordinates to the unhindered side.[12,27] On the other hand, A is also transformed into the $\mu$-peroxo and $\mu$-oxo dimers where the bridging ligands must reside on the unhindered side of the porphyrin. These transformations require that the dioxygen ligand be mobile, and this probably occurs through dioxygen dissociation. The availability of these five-coordinate[35,36] dioxygen adducts should make it

(31) The pyrrole resonances of both [T(2,4,6-MeO)$_3$PP]FeO$_2$ and [T-(2,4,6-EtO)$_3$PP]FeO$_2$ initially shift downfield upon warming before begining to shift upfield toward the position found for Fe$^{II}$. Similarly, the pyrrole resonance of [T(3,4,5-MeO)$_3$PP]FeO$_2$ shifts significantly downfield upon warming. These shifts could be caused by the presence of a third species, which could be a triplet form of PFeO$_2$. This point is under further investigation. There exists evidence for the existence of paramagnetic forms of hemoprotein dioxygen complexes.[32]

(32) Cerdonio, M.; Moraute, S.; Vitale, S. *Isr. J. Chem.* **1981**, *21*, 76–80.

(33) Wayland, B. B.; Mehne, L. F.; Sewartz, J. *J. Am. Chem. Soc.* **1978**, *100*, 2379–2383.

(34) Traylor, T. G.; Mitchell, M. J.; Tsuchiya, S.; Campbell, D. H.; Stynes, D. V.; Koga, N. *J. Am. Chem. Soc.* **1981**, *103*, 5234–5236. Traylor, T. G., personal communication.

(35) It seems unlikely that these oxygenated species have achieved hexacoordination at iron by intramolecular association. In the solid state [TpivPP]Fe$^{II}$(H$_2$O)SC$_4$H$_8$ is polymerized through coordination of the pivalamide oxygen to an iron atom of a different porphyrin.[36] In the $^1H$ NMR spectra of [TpivPP]FeO$_2$ there is no evidence of a unique set of *tert*-butyl resonances that would be associated with the unique, coordinated pivalamide group. For the iron complexes of the methoxy and ethoxy substituted porphyrins, there is no evidence for ether coordination in any oxidation state of the iron porphyrins. There exists the possibility that water, arising adventitiously, could occupy the sixth coordination site in these species. However, there is no evidence, specifically, no $^1H$ NMR resonance, for the presence of any sixth ligand.

possible to explore the effects of a wide variety of trans axial ligands on the properties of iron porphyrin dioxygen adducts; we have such studies in progress. The conversion of TpivPPFeO$_2$ into (*N*-MeIm)[TpivPP]FeO$_2$ not only shows that addition to the sixth site is possible, but it also interrelates the transient species observed here to a stable species that has been characterized by X-ray crystallography.

The paths of thermal decomposition of both [TpivPP]FeO$_2$ and [T(3,4,5-MeO)$_3$PP]FeO$_2$ are similar in that successive conversion to the peroxo- and oxo-bridged iron(III) porphyrins are observed. On the other hand, [T(2,4,6-MeO)$_3$PP]FeO$_2$ and [T(2,4,6-EtO)$_3$PP]FeO$_2$ are not transformed into peroxo- and oxo-bridged species upon warming. Undoubtedly this is a result of steric restraints that keep the two porphyrin too far apart to accommodate the requirements of the bridging ligand. Attempts to prepare PFeOFeP from these porphyrins by the reaction of PFeCl with hydroxide, generally a standard route to PFeOFeP,[29] produce only PFeOH.[16]

Warming [T(2,4,6-MeO)$_3$PP]FeO$_2$ or [T(2,4,6-EtO)$_3$PP]FeO$_2$ results in three reactions. The resonances of PFeO$_2$ and PFe$^{II}$ are in rapid exchange as shown by the data responsible for Figure 13. Thus dioxygen dissociation via eq 4 is occurring. Reversible dioxygen dissociation is also the simplest explanation for the rapid transfer of the dioxygen ligand from one side of the porphyrin plane to the other (eq 3). This process has been seen for both [T(3,4,5-MeO)$_3$PP]FeO$_2$ and [T(2,4,6-MeO)$_3$PP]FeO$_2$. However, our observations of this phenomenon have always been performed in the presence of excess dioxygen. More thorough kinetics study are necessary to distinguish between dissociative, associative, and interchange mechanisms. Additionally, PFeOH and PFeCl are produced as the final stable products of the reaction. Oxygenation of [T(2,4,6-MeO)$_3$PP]Fe$^{II}$ or [T(2,4,6-EtO)$_3$PP]Fe$^{II}$ at room temperature proceeds to form PFeOH and PFeCl without producing detectable quantities of PFeO$_2$. The chloride necessary for the formation of PFeCl must originate in the solvent. Superoxide ion is known to be highly reactive toward halocarbons and may be responsible for producing the chloride.[37] Superoxide could originate in this system by dissociation from PFeO$_2$, or PFeO$_2$ itself may display superoxide-like reactivity. Further investigation is necessary. Likewise, the source of the proton in PFeOH has not been identified. In fact, the entire process of conversion of PFeO$_2$ into PFeOH invites further study, which is underway in our laboratory.

Throughout this work, it has been assumed that the principal effect of phenyl ring substitution has been a steric one that limits dimer formation. Other consequences of such substitution, particularly electronic effects, remain to be elucidated. These may make other important contributions to the stability of PFeO$_2$. However, we do believe that the transient formation of diamagnetic PFeO$_2$ is likely for other iron(II) porphyrins when they are oxygenated under the conditions used here.[38]

---

(36) Jameson, G. B.; Robinson, W. T.; Collman, J. P.; Sorrel, T. N. *Inorg. Chem.* **1978**, *17*, 858–864.

(37) Roberts, J. L., Jr.; Sawyer, D. T. *J. Am. Chem. Soc.* **1981**, *103*, 712–714.

## Experimental Section

**Materials.** [T(2,4,6-MeO)$_3$PP]Fe$^{III}$Cl and [T(2,4,6-EtO)$_3$PP]Fe$^{III}$Cl were prepared by the procedure of Amundsen.[13] [TpivPP]H$_2$ was purchased from Man-Win Chemicals and converted to [TpivPP]Fe$^{III}$Br and [TpivPP]Fe$^{III}$OFe$^{III}$[TpivPP] by established procedure.[12] [T(3,4,5-MeO)$_3$PP]Fe$^{III}$Cl was prepared via standard procedures starting from 3,4,5-trimethoxybenzaldehyde.[39]

**Preparation of Samples for Spectroscopic Study.** Unligated iron(II) porphyrins were prepared by reduction of the appropriate iron(III) complex in toluene or dichloromethane solution with an aqueous sodium dithionite solution or zinc amalgam in a Kewannee controlled-atmosphere box under purified nitrogen. Typically 1 mg of iron(III) porphyrin and 5 mg of sodium dithionite were dissolved in a mixture of 0.5 mL of dichloromethane and several drops of water. The solutions were shaken to mix the two layers. After reduction was complete, as noted by a color change from green-brown to red, the two layers were allowed to separate. The aqueous layer was removed by a pipet. The dichloromethane solution was then washed with a fresh sample of deoxygenated water to remove any remaining inorganic salts. The dichloromethane was evaporated from the sample under vacuum, and the sample was dried for 12 h under continuous vacuum. The iron porphyrin was then dissolved in deoxygenated, deuterated dichloromethane and transferred into an NMR tube in the controlled atmosphere. The NMR tube was sealed with a septum cap. Other spectroscopic handling techniques have been described elsewhere.[19]

**Instrumentation.** $^1$H NMR spectra at 200 and 360 MHz were recorded on Nicolet NT-200 and NT-360 FT NMR spectrometers. Between 300 and 2000 transients were accumulated with the use of a 90° pulse. Electronic spectra were measured on a Cary 17 spectrometer equipped with a Kontes variable-temperature Dewar. The cuvette was cooled by immersion in a ethanol bath that was chilled by the addition of sufficient liquid nitrogen to reach −78 °C. Room-temperature electronic spectra were recorded on a Hewlett-Packard 8450A spectrophotometer.

**Registry No. 1**, 83198-46-3; **2**, 53470-07-8; **3**, 57018-42-5; **4**, 83136-57-6; **A**, 83136-58-7; **B**, 83136-62-3; **C**, 55272-38-3; **D**, 83136-61-2; **E**, 83136-63-4; **F**, 81278-78-6; **G**, 81245-19-4; [T(2,4,6-MeO)$_3$PP]FeO$_2$, 83136-59-8; [T(2,4,6-EtO)$_3$PP]FeO$_2$, 83136-60-1; [T(2,4,6-EtO)$_3$PP]Fe(CO)$_2$, 83136-64-5; [T(2,4,6-EtO)$_3$PP]Fe(CO), 83136-65-6; [T(3,4,5-MeO)$_3$PP]Fe(CO)$_2$, 83136-66-7; [T(2,4,6-MeO)$_3$PP]Fe$^{III}$Cl, 53470-05-6; [[T(2,4,6-EtO)$_3$PP]Fe(pip)$_2$]Cl, 83136-67-8; [T(2,4,6-EtO)$_3$PP]Fe$^{II}$(pip)$_2$, 83136-68-9; (*N*-MeIm)[TpivPP]FeO$_2$, 55449-22-4; [TpivPP]Fe$^{II}$(*N*-MeIm)$_2$, 75557-96-9; [T(2,4,6-EtO)$_3$PP]Fe$^{III}$Cl, 83136-69-0; [T(3,4,5-MeO)$_3$PP]Fe(CO), 83136-70-3; dioxygen, 7782-44-7; piperidine, 110-89-4; *N*-methylimidazol, 616-47-7; carbon monoxide, 630-08-0.

---

(38) (a) With [TPP]Fe$^{II}$, the formation of a diamagnetic species has been noted in some oxygenation experiments. This is particularly true when finely ground, solid [TPP]Fe$^{II}$ is dissolved at −70 °C in toluene that has been previously saturated with dioxygen. In such an experiment, the presence of excess dioxygen may inhibit peroxo dimer formation by reducing the availability of PFe$^{II}$. While these experiments are difficult to reproduce regularly, they are suggestive of the formation of [TPP]FeO$_2$. Chin, D. H., unpublished observations. (b) **Note Added in Proof:** The infrared spectrum of matrix isolated [TPP]FeO$_2$ has recently been reported: Nakamoto, K.; Watanabe, T.; Ama, T.; Urban, M. W. *J. Am. Chem. Soc.* **1982**, *104*, 3744–3745.

(39) Adler, A. D.; Longo, F. R.; Finarreli, J. F.; Goldmacker, J.; Assour, J.; Forskoff, L. *J. Org. Chem.* **1967**, *32*, 476.